



Modeling microtubule dynamic instability: Microtubule growth, shortening and pause

Frederick Laud Amoah-Darko Jr.¹, Diana White^{*,1}

Clarkson University, 8 Clarkson Avenue, Potsdam, NY, United States of America

ARTICLE INFO

Keywords:

Modeling microtubule dynamics
Paused state
MAPs
Hyperbolic systems
PDEs

ABSTRACT

Microtubules (MTs) are protein polymers found in all eukaryotic cells. They are crucial for normal cell development, providing structural support for the cell and aiding in the transportation of proteins and organelles. In order to perform these functions, MTs go through periods of relatively slow polymerization (growth) and very fast depolymerization (shortening), where the switch from growth to shortening is called a catastrophe and the switch from shortening to growth is called a rescue. Although MT dynamic instability has traditionally been described solely in terms of growth and shortening, MTs have been shown to pause for extended periods of time, however the reason for pausing is not well understood. Here, we present a new mathematical model to describe MT dynamics in terms of growth, shortening, and pausing. Typically, MT dynamics are defined by four key parameters which include the MT growth rate, shortening rate, frequency of catastrophe, and the frequency of rescue. We derive a mathematical expression for the catastrophe frequency in the presence of pausing, as well as expressions to describe the total time that MTs spend in a state of growth and pause. In addition to exploring MT dynamics in a control-like setting, we explore the implicit effect of stabilizing MT associated proteins (MAPs) and stabilizing and destabilizing chemotherapeutic drugs that target MTs on MT dynamics through variations in model parameters.

1. Introduction

Microtubules (MTs) are protein polymers found in all eukaryotic cells. They are crucial for many cellular processes including cell movement, cell differentiation, and cell division (Wade, 2009; Wollman et al., 2005; Etienne-Manneville, 2013). MTs are composed of 13 protofilaments constituted each by a longitudinal series of polarized α and β -tubulin heterodimers. As a result, MTs are polarized (Wade, 2009), where their “plus” and “minus” ends correspond to the ends where β - and α - tubulin dimers are mainly exposed, respectively, differing from each other according to chemical composition. These differences are often readily distinguished by their growing rates. Their plus ends grow more rapidly when both sides of the MT are exposed *in vitro* (Walker et al., 1988). Within animal cells, minus ends are nucleated by the centrosome (therefor are static) and MTs grow toward the cell periphery, with their plus ends being oriented toward the cell membrane, where GTP associated α - β -tubulin dimers are incorporated at the growing (active) end of the MTs, such that GTP hydrolysis occurs after addition. That is, after addition, and because elongation and GTP hydrolysis are not synchronized, a small GTP region can exist

at the growing front, referred to as the stabilizing GTP cap (Desai and Mitchison, 1997). The fine equilibrium that exists between the rate of GTP hydrolysis and that of the α - β -tubulin addition defines the stability of the MTs: when GTP-tubulin addition at the front end of the MT is faster than hydrolysis, the MT will continue to grow; when hydrolysis catches up with the growing front, the stabilizing GTP cap is lost and the MT quickly depolymerizes releasing free GDP-tubulin dimers. These GDP dimers are recycled back to free GTP-tubulin, which can be added back at the growing ends. The continual process of growth and shortening is referred to as *dynamic instability*.

Aside from growth and shortening, some experimental studies suggest that MTs may also undergo periods of pausing, and the reasons for this are largely unknown (Walker et al., 1988; van Riel et al., 2017; Trogden and Rogers, 2015; Moriwaki and Goshima, 2016). Consequently few studies have been carried out concerning the importance of the regulation of this dynamic state. Nevertheless, recent data suggests a broad role of the pause state for MT behavior and that the regulation of this state by cellular factors such as MT associated proteins (MAPs) may play essential roles in cellular physiology (Aureliana Sousa

* Corresponding author.

E-mail address: dtwhite@clarkson.edu (D. White).

URL: <https://www.dianawhitebiomath.com> (D. White).

¹ Both authors contributed equally to the preparation of this manuscript.

et al., 2007). Many computational and theoretical models have been developed to describe MT growth and shortening at the plus ends of MTs (Chen and Hill, 1985; Dogterom and Leibler, 1993; Flyvbjerg et al., 1994, 1996; Hinow et al., 2009; Martin et al., 1993; Mishra et al., 2005; Barlukova et al., 2018; White et al., 2017; Honore et al., 2019). To our knowledge, the only computational model which has been developed to explore MTs dynamics in terms of growth, shortening and pausing was proposed by Ebbinghaus and Santen (2011), where pausing occurs at the cell periphery where MAPs are linked to the “plus end” of MTs which are consequently stabilized before shortening. In addition, new work has shown, through high resolution microscopy and agent-based models, that the classical two-state model of growth and shortening does not adequately describe the more robust dynamics of MTs, and in particular the existence of a paused state (Mahserejian et al., 2022).

We propose a new mathematical model to take into consideration all the steps of the MT dynamic cycle (nucleation, growth, shortening and pause), where we assume MTs are non interacting for simplicity. This simplifying assumption is close to that defined *in vitro*, where MTs grow perpendicular from a barrier/plate in systems initially comprised of only $\alpha - \beta$ tubulin dimers (Dogterom and Leibler, 1993; Janson et al., 2003), or that of the classical centrosomal/astral configuration, exhibited in many cells. We model the time dependent distributions of growing, shortening, and pausing MTs using a system of three partial differential equations (PDEs). We couple this to a system of ordinary differential equations (ODEs) which describes the time evolution of free GTP- and GDP-tubulin concentrations. Similar to the work of Hinow et al. (2009), growth and shortening are described using advection-type processes. That is, we assume that MTs grow at a rate dependent on the free GTP-tubulin concentration, and that shortening occurs at a constant rate (independent of tubulin concentration), which is consistent with experimental studies under a given concentration of free tubulin Walker et al. (1988). Similar to White et al. (2017), an expression is derived, using the method of characteristics, to define time-based catastrophe frequency in the presence of pausing. In growth and shortening experiments (without pause), such catastrophe frequency is defined as the average number of shortening events (catastrophes) over the total time MTs spend in a period of growth. A similar definition which includes pausing has not been formalized in experiments. However, we suggest a similar definition to that proposed in Mahserejian et al. (2022); we suggest catastrophe frequency is the number of shortening events over the period of time MTs are in growth and pausing states.

The overview of the paper is as follows: in Section 2, we describe the model assumptions and develop a model for MT dynamics that accounts for MTs in growing, shortening, and pausing states, as well as free-tubulin populations. We derive a new expression for the MT catastrophe frequency in the presence of a paused state, as well as expressions for the total percentage of time that MTs spend in growing and paused states. In Section 3, we describe basecase simulation results for MT dynamics, using MT dynamic parameters taken from literature, and observe oscillating populations of tubulin in both free and polymerized form. In addition to exploring MT dynamics in a control-like setting (which we refer to as the basecase), we describe how variations in model parameters, such as the MT growth rate parameter, the number of transitions to a paused state, the MT shortening rate, and the MT hydrolysis rate, alter the MT dynamics in terms of the catastrophe frequency and the total time spent in a paused state. We describe how these results might be connected with the action of certain stabilizing/destabilizing MT associated proteins (MAPs), as well as certain classes of chemotherapeutic MT targeting drugs. Finally, in Section 4, we discuss the main results of our model simulations. One key result we show is that, by adding a small amount of pausing to the system, MT dynamics increases, as described by an increase in catastrophe frequency and stimulated oscillations.

2. Modeling framework

Here, we outline our model to describe MT dynamics in systems comprised solely of tubulin (free and polymerized forms). First, in Section 2.1, we outline the model assumptions, and then in Section 2.2, we provide details for the construction of the model based on the assumptions stated in Section 2.1.

2.1. Model assumptions

We first state model assumptions (A1) through (A7), and provide mathematical and biological reasoning for each:

(A1) MTs cannot grow below a critical GTP-tubulin concentration, above which the MT growth rate increases linearly with increasing GTP-tubulin concentration (this type of dynamics is observed experimentally (Walker et al., 1988)). Here $p(t)$ represents the GTP-tubulin concentration at time t , and the MT growth rate $\gamma^{poly}(p(t))$ is given by

$$\gamma^{poly}(p(t)) = \begin{cases} 0 & \text{when } p \leq p_c \\ \alpha(p(t) - p_c) & \text{when } p > p_c, \end{cases} \quad (1)$$

where α is the growth rate parameter and p_c is the critical tubulin concentration below which MTs cannot grow. A description of all model parameters, as well as ranges for their values, is found in Table 1.

(A2) MT hydrolysis is a complicated process, and there are a number of theories describing how the process might work. Coupled hydrolysis refers to the process by which hydrolysis is stimulated as soon as a GTP-tubulin dimer is added to a growing MT, while vectorial hydrolysis refers to the process by which hydrolysis is stimulated at the boundary between the GDP and GTP zone along a growing MT. Random hydrolysis (combined with coupled or vectorial hydrolysis) has also been considered (Bowne-Anderson et al., 2013; Walker et al., 1988). Since we make simplifying assumptions (described in the numerics section) to treat MTs as 1-D structures, we assume that the MT hydrolysis rate γ^h is kept constant and hydrolysis is a vectorial process which can be described mathematically using an advection (directed) term. Experimental ranges for γ^h are found in Table 1.

(A3) When the MT hydrolysis rate is smaller than the (time varying) MT growth rate, a MT continues to grow. When the hydrolysis rate is larger than the MT growth rate, a MT can undergo a *catastrophe event*, leading to MT shortening. The difference between the growth rate and the hydrolysis rate is denoted by $\gamma^{poly}(p(t)) - \gamma^h = R(t)$, for simplicity in notation, and describes the rate of change of the MT cap region.

(A4) MTs shorten at a constant rate δ . In experiments the shortening rate of MTs are found to be independent to changes in tubulin concentration (Walker et al., 1988; Fees and Moore, 2019).

(A5) MTs transition into the pausing state from the growing state with transition frequency C , which is defined as the average number of transitions MTs make to a paused state from a growth state over a specified period of time (typically the time frame of the simulation). Fewer transitions correspond to lower C , and many transitions corresponds to higher C . We define the number of pause transitions N_{tr} as

$$N_{tr} = C \times T_{sim},$$

where T_{sim} denotes the total simulation time. The parameter N_{tr} is adjusted based on the frequency C whose range is based on similar values found in Brittle and Ohkura (2005), as shown in Table 1.

(A6) We assume that MTs do not interact with each other and are only dynamic at their plus end. This simplifying assumption is representative of a system where MTs grow (mostly) perpendicular out from a barrier containing seeds for nucleation *in vitro*, similar to experiments completed by Janson et al. (2003), or systems where MTs grow out

Table 1
Table of model parameters, their ranges, and sources.

Parameter	Value
Critical tubulin concentration p_c	0–5 μM (Mirigian et al.; Walker et al., 1988)
Rescue propensity λ	3–10 min^{-1} (Honoré and Braguer, 2011)
Growth parameter α	0.5–15 $\mu\text{M}^{-1} \text{min}^{-1}$ (Walker et al., 1988; Hinow et al., 2009; Barlukova et al., 2018)
Hydrolysis rate γ^h	3–10 $\mu\text{m min}^{-1}$ (Barlukova et al., 2018; Hinow et al., 2009)
Shortening rate δ	3–36 $\mu\text{m min}^{-1}$ (Pagano et al., 2012; Walker et al., 1988; Fees and Moore, 2019)
Nucleation rate μ	$5.9 \times 10^{-3} \mu\text{M}^{-1} \text{min}^{-1}$ (Hinow et al., 2009)
GDP to GTP exchange rate κ	0.5–10 min^{-1} (Hinow et al., 2009)
Transition frequency C	0–1 min^{-1} [This paper]
Number of transitions N_{tr}	0–7.5 transitions [This paper]
Dimer nucleation number n	2–5 (Sept et al., 1999; Hinow et al., 2009)

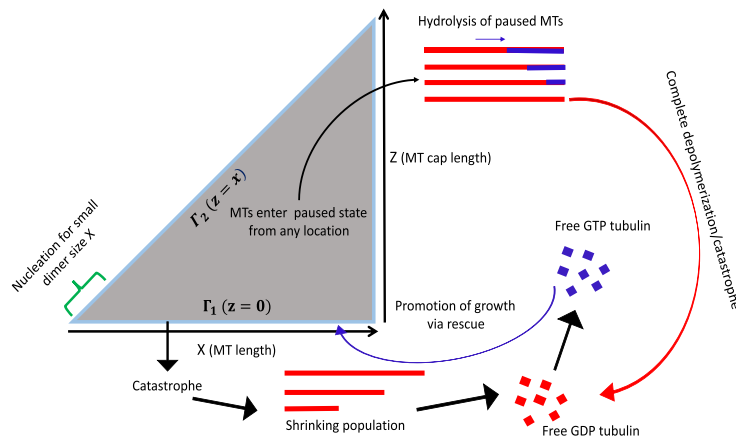


Fig. 1. Schematic representation of the MT dynamic cycle. MTs grow (along x -axis), and when they lose their cap ($z = 0$) they can undergo a catastrophe and shorten, releasing free-GDP tubulin back into the system. Free GDP-tubulin is recycled back into free-GTP tubulin and incorporated back into growing MTs via rescue. MTs can pause at any location in the domain, and completely depolymerize after losing their GTP cap in the paused state, entering into the free-GDP compartment.

radially from a centrosomal configuration (often called an astral array) *in vivo* (Dogterom and Leibler, 1993).

(A7) MTs can be rescued with frequency λ after depolymerization. Here, rescues are assumed to be independent of tubulin concentration (Fees and Moore, 2019), and are assumed to be end-driven (occurring closer to the MT nucleation site) and stochastic in nature. In a study by Fees and Moore (2019), the authors suggest that such rescue events, which are not well understood, are likely due to “lattice effects” or “GTP islands” that exist within the lattice, helping to promote rescue. The occurrence of such GTP islands, and mechanisms behind their existence have been studied by de Forges et al. (2016), and have been modeled by Honoré et al. (2019).

A schematic of the full model is given in Fig. 1. Here, the domain is described by the space spanned by the axes $x = 0$ and $x = z$ (a triangle). MTs are nucleated only when x is small (only a few dimers are needed for this process), and grow in length along direction x . Their GTP cap can grow or shrink along direction z , and when the cap size is zero, MTs enter the shortening compartment (if the hydrolysis rate exceeds the growth rate), where they undergo a complete catastrophe and enter the free-GDP-tubulin compartment, which is recycled back into free-GTP tubulin and added back to the growing MT population. An additional pause compartment is added to account for MTs that transition from growth to pause. Once in a paused state, hydrolysis always takes over the growth rate (as growth rate is zero), and MTs undergo a complete catastrophe when the GTP cap is lost, where polymerized tubulin becomes free GDP tubulin and the process repeats itself.

2.2. PDE model for polymerized tubulin populations

Here we describe the model formulation, where we use a PDE model, given by Eqs. (2), (3), and (4), to describe the time evolution of

growing MTs $u(x, z, t)$ of length x , cap size z , at time t , shortening MTs $v(x, t)$ of length x at time t , and pausing MTs $Q(x, z, t)$ of length x , cap size z , at time t .

The dynamics of growing MTs u are described by Eq. (2), where MT growth is described as an advection process such that MTs grow in the x direction at a rate $\gamma^{poly}(p(t))$, proportional to the GTP-tubulin concentration p (recall the description of MT growth described in (A1)). The MT cap size changes according to an advective process along the z direction, where the advection speed $R(t)$ is the difference between the growth rate $\gamma^{poly}(p(t))$ and the constant hydrolysis rate γ^h (i.e., $R(t) = \gamma^{poly}(p(t)) - \gamma^h$).

$$\frac{\partial u(x, z, t)}{\partial t} + \gamma^{poly}(p) \frac{\partial u}{\partial x} + (\gamma^{poly}(p) - \gamma^h) \frac{\partial u}{\partial z} = -Cu \quad (2)$$

$$\frac{\partial v(x, t)}{\partial t} - \delta \frac{\partial v}{\partial x} = - \begin{cases} \lambda v & \text{if } R(t) \geq 0 \\ R(t)u(x, 0, t) & \text{if } R(t) < 0 \end{cases} \quad (3)$$

$$\frac{\partial Q(x, z, t)}{\partial t} - \gamma^h \frac{\partial Q}{\partial z} = Cu, \quad (4)$$

The MT cap grows in direction z when $R(t) \geq 0$ and shortens when $R(t) < 0$. Finally, the term on the right side of Eq. (2) describes MTs that enter a paused state with transition frequency C . In other words, $-Cu$ is the rate of change of MTs out of the growing state u and into the paused state Q .

The dynamics of shortening MTs v are described by Eq. (3), where MTs shorten at a constant rate δ along the x direction, and can be rescued at a rescue frequency λ (entering back to the growing state via a boundary condition described in Section 2.2.1). Further, growing MTs that undergo a catastrophe (have cap size $z = 0$ when $R(t) < 0$) enter the shortening state.

Finally, the dynamics of pausing MTs Q are described by Eq. (4), where MTs enter the paused state from the growing state at rate Cu . In the paused state, the MT length remains fixed at the length

x at which it entered this state, and the MT cap size z shortens at the constant hydrolysis rate γ^h . Since paused MTs can only undergo hydrolysis (they do not grow), we assume that MTs remain in the pausing state until they lose their stabilizing GTP cap. Once that happens a complete catastrophe occurs (MT shorten instantaneously) and the MT completely depolymerizes to free GDP-tubulin, entering the free GDP-tubulin state q as described by Eq. (11) in what follows.

2.2.1. Boundary conditions for PDE system

We define the boundary conditions for the PDEs given by Eqs. (2), (3), and (4) by considering the state space $\Sigma = \{(x, z) \in \mathbb{R}^2 : x \geq z \geq 0\}$ with boundaries $\Gamma_1 = \{(x, z) \in \Sigma : z = 0\}$ and $\Gamma_2 = \{(x, z) \in \Sigma : x = z\}$. The schematic of the domain, including these boundaries, is described in Fig. 1.

On the boundary Γ_2 , we define a **nucleation boundary condition** for growing MTs u . In particular, we define the condition

$$\gamma^h u(x, x, t) = \frac{\mu p^n \xi(x)}{L^*}, \tag{5}$$

where the rate of nucleation is given by $\mu > 0$ (Hinow et al., 2009), n refers to the number of tubulin heterodimers needed for nucleation (we set $n=2$, as this is the smallest number of tubulin dimers required for nucleation), and the function $\xi(x)$ is the length distribution of freshly nucleated MTs, approximated by a heavy side function that is non-zero for small MT length x such that

$$\xi(x) = 1 - H(x, x_{max}). \tag{6}$$

We define nucleation in this way since newly formed MTs consist of a very small number of tubulin dimers (Sept et al., 1999). Parameter x_{max} describes the largest length of a freshly nucleated MT, where we set $x_{max} = 0.5 \mu\text{m}$ (which corresponds to 1 grid cell in our simulation domain, as described later in the numerical details section). Finally, the average length of nucleated MTs is given by

$$L^* = \int_0^\infty \xi(x) x dx. \tag{7}$$

Along the boundary Γ_2 we prescribe a no-flux condition for pausing MTs Q such that MTs cannot grow past the boundary x (i.e., tubulin is not lost, but is conserved in our system).

$$\left. \frac{\partial Q(x, z, t)}{\partial z} \right|_{z=x} = 0 \tag{8}$$

Finally, we consider the boundary Γ_1 when $R(t) \geq 0$. Along this boundary we describe a **rescue boundary condition** for u , such that MTs that do not have GTP cap are rescued according to the boundary condition

$$R(t)u(x, 0, t) = \lambda v(x, t) \text{ for } R(t) \geq 0. \tag{9}$$

Parameter λ refers to the rescue frequency at which shortening MTs re-enter the growing state (Hinow et al., 2009; White et al., 2017).

2.3. ODE model for free-tubulin populations

The temporal dynamics of the free-GTP tubulin $p(t)$ and free-GDP tubulin $q(t)$ concentrations are described by Eqs. (10) and (11), respectively. These equations are formulated from a conservation law, such that the total tubulin in the system (free and polymerized) remains constant. In other words, the PDEs given by Eqs. (2) through (4) are transformed to ODEs (describing concentrations of tubulin in polymer form over time), by multiplying each equation by x (representative of polymer length) and integrating over the state space. The new terms that come out of this integration are included into the ODE system given by Eqs. (10) and (11) in such a way as to conserve the total tubulin concentration. A full derivation of the 5-dimensional ODE system is given in the Appendix and is analogous to work completed by (Hinow et al., 2009).

$$\frac{dp}{dt} = -\gamma^{poly}(p) \int_0^\infty \int_0^x u(x, z, t) dz dx - \mu p^n + \kappa q \tag{10}$$

$$\frac{dq}{dt} = \delta \int_0^\infty v(x, t) dx - \kappa q + \gamma^h \int_0^\infty Q(x, 0, t) x dx \tag{11}$$

The first term on the right-hand side of Eq. (10) describes the uptake of free-GTP tubulin p as a MT grows, while the second term describes free-GTP tubulin used in the nucleation process. The final term is added to describe the exchange of free-GDP tubulin to free-GTP tubulin, where κ describes the rate of biochemical pumping as GDP tubulin is converted to GTP tubulin. Finally, the first term in Eq. (11) describes all free-GDP tubulin q that comes from a shortening event while the second term describes the GDP/GTP exchange. The last term in Eq. (11) describes the free-GDP tubulin that comes from the pause state Q (those paused MTs that have lost their GTP cap such that $z = 0$). All model parameters, their values, and sources are summarized in Table 1.

2.4. Calculating catastrophe frequency f_c when paused state incorporated

In previous works, the key dynamic parameters that help to describe MT dynamics include (1) the catastrophe frequency, (2) the rescue frequency, (3) the MT growth rate, and (4) the MT shortening rate. In our model, the MT shortening rate δ and rescue frequency λ are model inputs and specified at the beginning of a simulation. In addition, the MT growth rate $\gamma^{poly}(p)$ is dependent on the free-GTP tubulin population p , as described by Section 2.1. Here, we expand on the work of White et al. (2017) to include a pausing state, for which we include new dynamic parameters, specifically we include (1) the transition to pause frequency C , and a new expression for the catastrophe frequency \tilde{f}_c that incorporates both catastrophe from growth and paused states.

In White et al. (2017), the authors derive a mathematical definition for catastrophe frequency, which is based on an experimental definition for catastrophe frequency in the absence of pause as outlined by Walker et al. and others (Walker et al., 1988). In particular, time-based catastrophe for a single MT is described as:

$$f_c = \frac{\text{the number of catastrophe events}}{\text{total time for which a MT spends in the growing state}}$$

For this experimental description, the mean catastrophe frequency is calculated by averaging over the catastrophe frequencies for many MTs within a single experiment.

Fig. 2(a) illustrates a schematic of a single MT growing and shortening over time, and Fig. 2(b) illustrates a single MT growing, pausing, and shortening over time. Here, we highlight a MT undergoing 3 catastrophe events over a given time period, where the t_i 's correspond to growing times and the \tilde{t}_i 's correspond to the pausing times. From Fig. 2(a), and using the experimental definition for catastrophe frequency in the absence of pause we arrive at the catastrophe frequency

$$f_c = \frac{3}{t_1 + t_2 + t_3}$$

Currently, there is no common consensus for a similar definition of catastrophe frequency in the presence of pause. However, using the above definition as motivation for a new description, and similar to the work of Mahserejian et al. (2022), we suggest that such a definition would take on the form

$$\tilde{f}_c = \frac{3}{t_1 + t_2 + t_3 + \tilde{t}_1 + \tilde{t}_2 + \tilde{t}_3}.$$

To determine the growing times and pausing times from our model, we make use of the method of characteristics as applied to the pair of hyperbolic PDEs (2) and (3) for growing and pausing MTs, respectively. For ease in reading we write them again here:

$$\begin{aligned} \frac{\partial u(x, z, t)}{\partial t} + \gamma^{poly}(p(t)) \frac{\partial u(x, z, t)}{\partial x} + (\gamma^{poly}(p(t)) - \gamma^h) \frac{\partial u(x, z, t)}{\partial z} &= -Cu \\ \frac{\partial Q(x, z, t)}{\partial t} - \gamma^h \frac{\partial Q}{\partial z} &= Cu, \end{aligned}$$

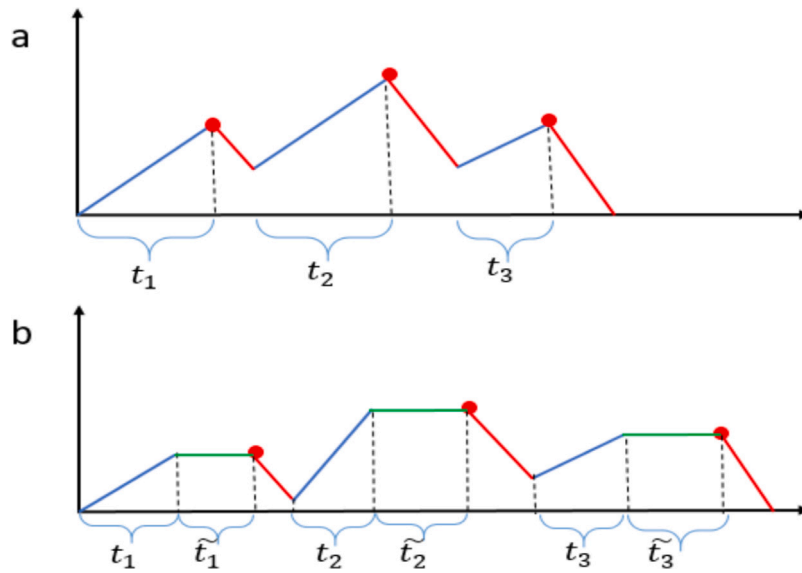


Fig. 2. Schematic of MT growth over time. MT length is depicted along the y-axis, while time is along the x-axis. (a) MT length over time with no pause; (b) MT length over time with pause. The blue lines illustrate time periods for which a MT spends growing (indicated by times t_i), the green lines refer to time periods for which a MT pauses (indicated by times \tilde{t}_i), and the red dots correspond to catastrophe events.

From the above equation of growth u , the characteristic equation for MT-cap size z is

$$\frac{dz}{dt} = R(t), \quad (12)$$

Where we recall that $R(t) = \gamma^{poly}(p(t)) - \gamma^h$. Solving this equation for $z(t)$ gives

$$z(t) = z(t_0) + \int_{t_0}^t R(s)ds. \quad (13)$$

where $z(t_0)$ is the “initial” value for z , and we consider this to be the time at which a *rescue* takes place such that $R(t) \geq 0$ and $z(t_0) = 0$. Now, since we know a *catastrophe* would occur at a later time \bar{t} where $R(t) < 0$ and $z(\bar{t}) = 0$, starting at the rescue time t_0 we trace forward along the characteristic curve $z(t)$ to the catastrophe time \bar{t} . Substituting $z(t_0)$ and $z(\bar{t})$ into (13) we arrive at

$$z(\bar{t}) - z(t_0) = \int_{t_0}^{\bar{t}} R(s)ds \quad (14)$$

and since $z(t_0) = z(\bar{t}) = 0$, we have

$$\int_{t_0}^{\bar{t}} R(s)ds = 0. \quad (15)$$

Numerically solving this integral gives us the mean growing time

$$T_{grow}(\bar{t}) = \bar{t} - t_0, \quad (16)$$

where catastrophe events happen at time \bar{t} . To determine the total grow time of MTs over the entire time course of the simulation (T_{sim}) we write

$$\bar{T}_{grow} = \int_0^{T_{sim}} T_{grow}(\bar{t})d\bar{t}. \quad (17)$$

Next, we determine the pausing time, which we will denote as T_{pause} . From the pausing equation for Q the characteristic equation for cap size z is

$$\frac{dz}{dt} = -\gamma^h. \quad (18)$$

Solving this equation using an initial condition $z(0) = z(t^*)$, where t^* is the time a MT enters the pause state we arrive at

$$z(t) = z(t^*) + \int_{t^*}^t -\gamma^h ds, \quad (19)$$

where $z(t) - z(t^*)$ is the length of the MT GTP cap at some time t after entering the pause state at time t^* . Since MTs only exit the pause state when the cap size $z = 0$, we define $z(t_{exit}) = 0$ at exit time t_{exit} and write

$$z(t^*) = \int_{t^*}^{t_{exit}} \gamma^h ds, \quad (20)$$

where we define the MT pause time as

$$T_{pause}(t^*) = t_{exit} - t^*.$$

Since

$$z(t^*) = (t_{exit} - t^*)\gamma^h,$$

as γ^h is constant, we arrive at the expression

$$T_{pause}(t^*) = z(t^*)/\gamma^h. \quad (21)$$

To determine the total pause time over the entire time course of the simulation (T_{sim}) we write

$$\bar{T}_{pause} = \int_0^{T_{sim}} T_{pause}(t^*)dt^*. \quad (22)$$

Finally, we derive a new definition of catastrophe frequency for those MTs that undergo catastrophe directly from a growing state when their cap size is zero and $R(t) < 0$, and those that undergo catastrophe from a paused state after losing their stabilizing GTP cap. As described above, we define the *catastrophe frequency with pause* as the sum of the catastrophes that occur after growing and those that occur after pausing, divided by the total time a MT spends in either the growing or pausing state. If we define A as the total number of catastrophes from a growing state and B as the total number of catastrophes from a paused state, the time-based catastrophe frequency with pause is given by,

$$\bar{f}_c = \frac{\int_0^{T_{max}} \frac{1}{T_{grow}(t) + T_{pause}(t)} (A + B)dt}{\int_0^{T_{max}} (A + B)dt} \quad (23)$$

where

$$A = \int_0^\infty u(x, 0, t)dx, \quad \text{when } R(t) < 0, \quad (24)$$

$$B = \int_0^\infty Q(x, 0, t)dx, \quad (25)$$

such that $u(x, 0, t)$ is the number density of MTs that undergo a catastrophe from the growing state with cap size $z = 0$ and $Q(x, 0, t)$ is the number density of MTs that undergo a catastrophe from the paused state with cap size $z = 0$.

3. Results

3.1. Numerical details and initial/baseline simulations

We simulate our model using a finite volume method. For the advection terms in Eqs. (2) to (4) we use an upwinding approach, while for the ODEs (12) and (11) we use an explicit Euler strategy. All simulations are implemented in Matlab using custom code similar to that outlined in [Barlukova et al. \(2018\)](#). We discretize our domain into 1000×1000 cells, where each cell has a dimension of $200 \text{ nm} \times 200 \text{ nm}$. Because the MT growth rate changes in time we use an adaptive time step (with a maximum time step of 0.1) to ensure that our scheme satisfies the CFL condition ([Zauderer, 2006](#)). The quantities for free GTP and GDP-tubulin (p and q) are measured in μM (1 micromole per liter), and the length of a MT and its' GTP cap region are measured in μm . Similar to [Hinow et al. \(2009\)](#), we define a conversion factor to represent μM in terms of μm , so that all units are consistent. In particular, in $1 \mu\text{mol}$ of tubulin, there are $N_A \times 10^{-6}$ molecules of tubulin, where $N_A = 6.022 \times 10^{23}$ is Avogadro's number. For simplicity, we assume a MT is one-dimensional, where in reality most MTs are composed of 13 protofilaments. Thus, we estimate the length of one dimer in our model, l_{unit} , to be the true length of a dimer divided by 13. That is,

$$l_{unit} = \frac{8.12 \times 10^{-3}}{13} \mu\text{m}.$$

Thus, the factor of conversion from μM to μm is

$$conv = 6.022 \times 10^{17} \times l_{unit}.$$

For the complete system of equations given by Eqs. (2), (3), (4), (10), and (11), we simulate our model using the following initial conditions:

$$u(x, z, 0) = 0$$

$$v(x, 0) = 0$$

$$Q(x, z, 0) = 0$$

$$p(0) = 15 \mu\text{M}$$

$$q(0) = 0.$$

That is, we assume our system is initially comprised of only free GTP-tubulin, such that MT dynamics are initiated through the process of nucleation. Since the polymer populations include descriptions for length, we convert each to tubulin concentrations by multiplying each polymer equation through by the tubulin length x and integrate over the state space to give:

$$\bar{u}(t) = \int_0^\infty \int_0^x u(x, z, t) x dz dx = \text{Total tubulin in growing MTs,}$$

$$\bar{v}(t) = \int_0^\infty v(x, t) x dx = \text{Total tubulin in shortening MTs,}$$

and

$$\bar{Q}(t) = \int_0^\infty \int_0^x Q(x, z, t) x dz dx = \text{Total tubulin in pausing MTs.}$$

By converting the polymerized system described by PDEs to an ODE system describing tubulin concentrations over time, we can illustrate the full system in terms of tubulin concentrations for both polymer populations and free-tubulin populations. The calculation to convert

Table 2

Table of time dependent state variables.

Variable	Meaning
$\bar{u}(t)$	Concentration of tubulin in growing MTs at time t (μM)
$\bar{v}(t)$	Concentration of tubulin in shrinking MTs at time t (μM)
$\bar{Q}(t)$	Concentration of tubulin in pausing MTs time t (μM)
$p(t)$	Free GTP-tubulin concentration at time t (μM)
$q(t)$	Free GDP-tubulin concentration at time t (μM)

Table 3

Basecase model parameters for simulations shown in [Fig. 3](#).

Parameter	SI units	Baseline value
p_c	μM	2
λ	min^{-1}	0.136
α	$\mu\text{m min}^{-1} \mu\text{M}^{-1}$	2.5
γ^h	$\mu\text{m min}^{-1}$	6
δ	$\mu\text{m min}^{-1}$	20
μ	$\text{M}^{-1} \text{min}^{-1}$	5.9×10^3
κ	min^{-1}	1
C	min^{-1}	0 or 0.1
N_{ir}	Dimensionless	0 or 1.5
Dimer nucleation number n	Dimensionless	2

to the ODE system is given in [Appendix](#), and uses a key assumption that the total tubulin in the system is conserved. [Table 2](#) summarizes all model variables for each tubulin population. These time dependent variables will be those illustrated in the plots that follow.

To understand how tubulin concentrations in each of polymerized and free form evolve with time, we illustrate their temporal dynamics in [Fig. 3](#) using the parameter values summarized in [Table 3](#) (which are from the experimental ranges given in [Table 1](#)).

[Fig. 3](#) illustrates that tubulin concentrations oscillate over time, highlighting the classical switch between growing (red curve) and shrinking (blue) states. In [Fig. 3\(left\)](#), we illustrate a system with no pause (transition to pause state number $N_{ir} = 0$), and in [Fig. 3\(right\)](#) we add a small transition to the pause state from the growing state ($N_{ir} = 1.5$). In both cases, the system dynamics are similar in that each are initially comprised of $15 \mu\text{M}$ of free-GTP tubulin (green curve), which immediately drops off as it is used to promote nucleation and then MT growth. The tubulin concentration in the growth state starts early on (described by the red curve), peaking at about 3 min and then settling into an oscillatory state. Following the initial period of growth, tubulin enters the shortening state (described by the dark blue curve) as depolymerization occurs due to GTP hydrolysis and subsequent catastrophe. Directly after entering the shortening state the tubulin enters the free-GDP tubulin state (described by the cyan curve) and GDP is quickly converted back to free GTP-tubulin (described by the green curve). Due to the positive (non-zero) rates of nucleation (μ), pumping (κ), and rescue frequency (λ), we do not see complete depletion of tubulin from the polymerized states, and in fact we see sustained oscillations, which is characteristic of many MT systems. If, for example, the rescue frequency was set to zero, the system would eventually break down into just free-GTP and free-GDP tubulin (result not shown here, but a similar result is described in [Hinow et al. \(2009\)](#)). Also, we observe that the addition of pause, added by setting the pausing transition to $N_{ir} = 1.5$ from $N_{ir} = 0$ ([Fig. 3\(right\)](#)), stimulates MT dynamics in the sense that the tubulin populations oscillate with greater frequency (paused state shown by black curve) and the catastrophe frequency increases from close to zero to $\tilde{f}_c = 1.6354 \text{ min}^{-1}$. This gives an indication that small pause transition numbers N_{ir} might play an important role in MT dynamics in the sense that MT dynamics are stimulated (as shown by increased oscillations in the tubulin concentration curves and the increase in the catastrophe frequency). We should note that different basecase parameter sets tested give different catastrophe frequencies, but the same qualitative features hold when increasing N_{ir} from zero across

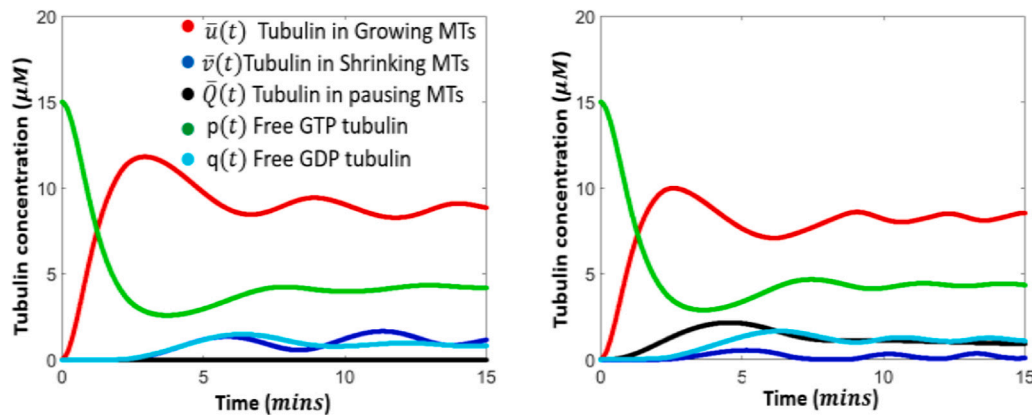


Fig. 3. Time evolution of tubulin concentration in growing \bar{u} , shrinking \bar{v} , pausing \bar{Q} , and free tubulin 4 states p and q (units in μM) for the baseline parameters described in Table 3. Left: $N_{tr} = 0$ (no pause) and catastrophe frequency \bar{f}_c is near 0 ($3.434 \times 10^{-7} \text{ min}^{-1}$). Right: pausing transition is $N_{tr} = 1.5$ and catastrophe frequency $\bar{f}_c = 1.6354 \text{ min}^{-1}$. Here we note that MTs oscillate between different populations in each case, where the frequency of oscillations increases slightly when pausing is incorporated to the system.

all these parameter sets. That is, increasing the number of pausing transitions from $N_{tr} = 0$ to $N_{tr} = 1.5$ always results in a significant increase in catastrophe frequency and an increase in the frequency of oscillations in the tubulin concentration curves (results not shown).

3.2. Implicit effect of MAPs and MT chemotherapeutic drugs on MT dynamics

We examine how the incorporation of a pausing state into our model changes the model dynamics (where initially we set the number of transitions to the paused state $N_{tr} = 0$). In addition to varying the pausing frequency, we also look at how variations in the growth rate parameter α , the shortening rate δ , and the hydrolysis rate γ^h , alter MT dynamics in terms of (A) the catastrophe frequency \bar{f}_c derived in Eq. (23), and (B) the percentage of time that the MTs spend in each of the growing and pausing states (determined by knowing the grow time \bar{T}_{grow} in Eq. (17), the pause time \bar{T}_{pause} in Eq. (22), and the total simulation time T_{sim}). Our hope is that such variations will provide details into the implicit action of certain MT associated proteins (MAPs) and chemo drugs that work to alter the dynamics on MTs *in vitro* and *in vivo* (Stanton et al., 2011; Zhou and Giannakakou, 2005; Hamel et al., 1981; Kumar, 1981; Mishra et al., 2005; Zhou and Giannakakou, 2005; Berges et al., 2014). This will be described in further detail in the next two subsections.

3.2.1. Exploring MT stabilization: varying the transition to pause number N_{tr} and growth rate parameter α

Groups of MAPs that act as MT stabilizers (examples include +TIPs, MT plus-end tracking proteins) are known to specifically bind to growing MT plus ends to promote polymerization and stabilization (Stanton et al., 2011). MT stabilizing drugs include drugs that bind to the taxane site, including paclitaxel (taxol), docetaxel (taxotere), and taxol analogs (Stanton et al., 2011; Zhou and Giannakakou, 2005). These drugs are commonly used as cytotoxic agents targeting a variety of tumors. Their cytotoxic effect has been attributed to their ability to bind to tubulin and stabilize protofilaments, which leads to MT over-polymerization, and ultimately cell death. Not only do the addition of such drugs decrease catastrophe frequency and increase pause time (like +TIPs described above), but their addition often results in an overall shorter population of polymerized MTs (Hamel et al., 1981; Kumar, 1981).

As stabilizing MAPs and chemo drugs for MTs have the effect of promoting polymerization and stabilization, which is similar to how we expect increases in the growth rate parameter α and increases in the pause transition number N_{tr} to act on MTs, we vary both these parameters and see exactly what influence they have on MT dynamics.

Table 4

Table showing the amount of time tubulin in polymer form spends in a paused and a growing state for an increase in the pause transition number N_{tr} . All other parameters fixed to the basecase parameter set in Table 3.

Percentage of time spent in growing and pausing states					
	$N_{tr} = 1.5$	$N_{tr} = 3$	$N_{tr} = 4.5$	$N_{tr} = 6$	$N_{tr} = 7.5$
Pause	3.43	7.2224	11.0418	14.0816	16.2356
Grow	89.34	74.5274	40.2019	22.4126	9.0401

Table 5

Catastrophe frequency \bar{f}_c for varying growth rate parameter α and transition number N_{tr} .

	Catastrophe frequency				
	$N_{tr} = 1.5$	$N_{tr} = 3$	$N_{tr} = 4.5$	$N_{tr} = 6$	$N_{tr} = 7.5$
$\alpha = 2$	1.1868	1.6596	0.8436	0.8917	1.0614
$\alpha = 2.5$	1.6354	1.1348	0.7537	0.7927	0.9207
$\alpha = 3.0$	1.0896	1.5987	0.6919	0.7253	0.8096
$\alpha = 3.5$	1.0891	0.6461	0.6496	0.6710	0.7369

Later we include a discussion of the implicit action of such stabilizers (MAPs and drugs) on MT dynamics.

In Table 4 we highlight the total time for which MTs spend in growing and pausing states, for changes in the pause transition number N_{tr} . In particular, increases in N_{tr} lead to an increase in the pausing time, and a reduction in the amount of growing time, which is similar to the action of MT stabilizing drugs and MAPs. These results are further illustrated by looking at the corresponding curves for tubulin concentration over time for increasing N_{tr} in Fig. 4.

In Fig. 4, we show that the growing tubulin population decreases (red curve), while the pausing population increases (black curve), as read from the top left to the bottom right figure pane. It is interesting to note that for N_{tr} very large, there are few (almost zero) MTs in the shortening state (blue curve), shown by the bottom two panes in the figure. This likely has to do with the model construction (when pausing transition frequency is increased, more MTs leave the growing state to go to the paused state, leaving fewer MTs the opportunity to lose their GTP cap and enter the shortening state). In addition, if we look at the free GTP and GDP populations at the end of the simulation (at 15 min, green and cyan curves, respectively), the addition of these two populations are very similar for low vs high N_{tr} (varying from $\approx 5 \mu\text{M}$ to $\approx 6.5 \mu\text{M}$), which suggests that total tubulin in polymer form decreases slightly.

Next we explore the catastrophe frequency given by Eq. (23) and the percentage of time MTs spend in a paused state using Eq. (22) as we vary the transition to pause number N_{tr} and the growth parameter

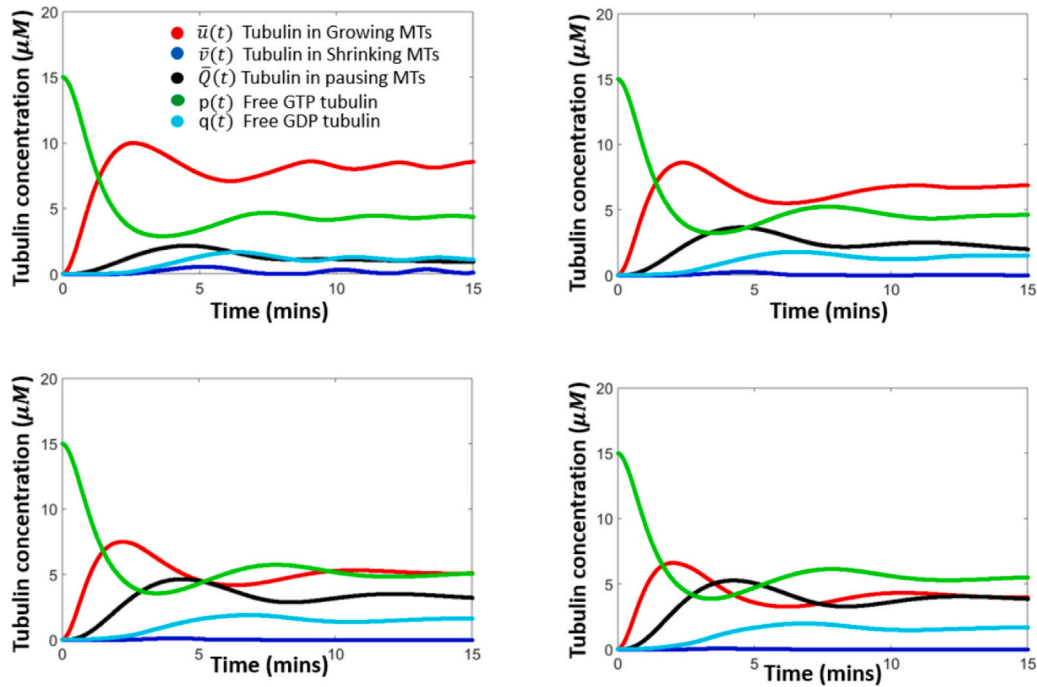


Fig. 4. Time evolution of tubulin concentration in growing \bar{u} , shrinking \bar{v} , pausing \bar{Q} , and free tubulin states p and q (units in μM) for the baseline parameters described in Table 3 for variation in the transition to pause number N_{tr} . Top left, $N_{tr} = 1.5$; Top right, $N_{tr} = 3$; bottom left, $N_{tr} = 4.5$; bottom right, $N_{tr} = 6$. The total tubulin in the growing state decreases (red curve), and the total tubulin in the paused state increases (black curve), as we move from the top left to the bottom right pane in the figure. In addition the total free tubulin (green and cyan curves) in the system increases slightly (from $\approx 5 \mu\text{M}$ to $\approx 6.5 \mu\text{M}$).

Table 6

Pause duration (as a percent of simulation time) for varying growth rate parameter α and transition number N_{tr} .

	Pause duration (% of Simulation time)				
	$N_{tr} = 1.5$	$N_{tr} = 3$	$N_{tr} = 4.5$	$N_{tr} = 6$	$N_{tr} = 7.5$
$\alpha = 2$	2.2227	4.647	7.258	9.6027	11.356
$\alpha = 2.5$	3.43	7.2227	11.042	14.0813	16.2353
$\alpha = 3.0$	4.664	9.783	14.54	18.108	20.5747
$\alpha = 3.5$	5.8873	12.2027	17.6773	21.656	24.373

α . From Table 5 we note that for a fixed pause transition number N_{tr} , increasing α has the effect of decreasing the catastrophe frequency (see first column in Table 5 highlighted in cyan, for example), and we note that MTs remain in a state of pause longer as α is increased (see the first row in Table 6 highlighted in cyan). Both these features are again qualitatively similar to the effects of certain classes of MAPs and MT stabilizing drugs on MT dynamics.

In Fig. 5 we show the time evolution of the tubulin populations for fixed $N_{tr} = 1.5$ and increasing α . Here we note the suppression of MT dynamics (shown by flattening of the polymerized MT population curves in red, black, and blue), where the paused MT population size increases (black curves). This is consistent with the increase in pause duration noted in Table 6. Here we note that, unlike changes in N_{tr} , our model predicts that less free tubulin is in the system as α is increased, where the free tubulin ranges from $7\mu\text{M}$ in the first figure pane (top left) and is reduced to $\approx 4.5\mu\text{M}$ in the bottom right figure pane. Unlike the previous case, there is an increase in polymerized tubulin for increasing N_{tr} , whereas there is a decrease in polymerized tubulin for increasing α . This results could be suggestive that the growth rate parameter is implicitly effected by stabilizing MAPs (Stanton et al., 2011) (promoting MT growth and stabilization), while pause transition number N_{tr} might be implicitly acted on by the stabilizing chemo drugs since certain drugs like those from the taxan family act in a way which usually results in an overall shorter population of polymerized MTs (Hamel et al., 1981; Kumar, 1981).

Table 7

Catastrophe frequency \bar{f}_c for varying shortening rate δ and transition number N_{tr} .

	Catastrophe frequency				
	$N_{tr} = 1.5$	$N_{tr} = 3$	$N_{tr} = 4.5$	$N_{tr} = 6$	$N_{tr} = 7.5$
$\delta = 15$	1.1404	1.1019	0.7518	0.7908	0.9186
$\delta = 20$	1.6354	1.1348	0.7537	0.7927	0.9207
$\delta = 25$	1.2611	1.1485	0.7534	0.7935	0.9205
$\delta = 30$	1.1098	1.1624	0.7537	0.7929	0.9228

Table 8

Pause duration (as a percent of simulation time) for varying shortening rate δ and transition number N_{tr} .

	Pause duration (% of Simulation time)				
	$N_{tr} = 1.5$	$N_{tr} = 3$	$N_{tr} = 4.5$	$N_{tr} = 6$	$N_{tr} = 7.5$
$\delta = 15$	3.4075	7.2194	11.0392	14.0813	16.2356
$\delta = 20$	3.4300	7.2224	11.0418	14.0816	16.2356
$\delta = 25$	3.4428	7.2218	11.0424	14.0813	16.2354
$\delta = 30$	3.4511	7.2206	11.0425	14.0809	16.2351

3.2.2. Exploring MT destabilizing: varying the transition to pause number N_{tr} , the MT shortening rate δ , and the hydrolysis rate γ^h

Examples of chemo drugs that act as MT destabilizers are those from the vinca alkaloid family, which include vinblastine and vincristine, and the drug colchicine (Mishra et al., 2005; Zhou and Giannakakou, 2005; Berges et al., 2014). At high concentrations, the vinca alkaloids have affinity for free tubulin heterodimers, which potentially form altered/curved tubulin dimers which cannot be added to a growing MT. Also, at high concentrations, colchicine promotes MT depolymerization, possibly through increases in the hydrolysis rate (Mishra et al., 2005; Zhou and Giannakakou, 2005; Berges et al., 2014).

As destabilizing chemo drugs for MTs have the effect of depolymerization, we expect that increases in the MT shortening rate δ and the MT hydrolysis rate γ^h might influence MTs dynamics in a similar way as these destabilizing drugs. Hence, we might gain insight into the potential implicit actions that these drugs have on such

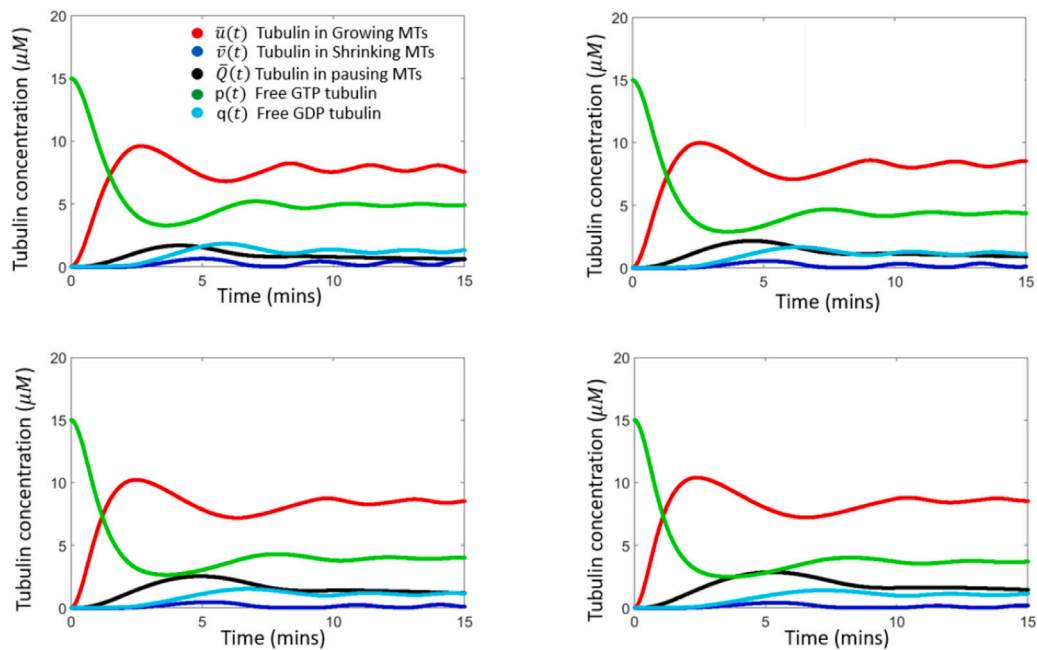


Fig. 5. Time evolution of tubulin concentration in growing \bar{u} , shrinking \bar{v} , pausing \bar{Q} , and free tubulin states p and q (units in μM) for the baseline parameters described in Table 3 for variation in the growth rate parameter α . Top left, $\alpha = 2$, top right, $\alpha = 2.5$, bottom left, $\alpha = 3$ and bottom right, $\alpha = 3.5$. Shown here are the total amounts of tubulin in each state (growing \bar{u} , shrinking \bar{v} , pausing \bar{Q} , along with free tubulin populations (units in μM). The number of pause transitions $N_{tr} = 1.5$ is held constant. As α increases, MT dynamics are dampened as we see a decrease in oscillations in the state curves.

Table 9
Catastrophe frequency f_c for varying hydrolysis rate γ^h and transition number N_{tr} .

	Catastrophe frequency				
	$N_{tr} = 1.5$	$N_{tr} = 3$	$N_{tr} = 4.5$	$N_{tr} = 6$	$N_{tr} = 7.5$
$\gamma^h = 4$	0.7863	0.4824	0.4926	0.5397	0
$\gamma^h = 6$	1.6354	1.1348	0.7537	0.7927	0.9207
$\gamma^h = 8$	1.7839	1.8389	2.0398	1.0678	1.1349
$\gamma^h = 10$	1.6516	1.9905	2.7544	2.3057	1.395

Table 10
Pause duration (as a percent of simulation time) for varying hydrolysis rate γ^h and transition number N_{tr} .

	Pause duration (% of Simulation time)				
	$N_{tr} = 1.5$	$N_{tr} = 3$	$N_{tr} = 4.5$	$N_{tr} = 6$	$N_{tr} = 7.5$
$\gamma^h = 4$	13.5938	25.4627	33.9754	39.4988	43.0941
$\gamma^h = 6$	3.4300	7.2224	11.0418	14.0816	16.2356
$\gamma^h = 8$	1.0693	2.2597	3.5314	5.0146	6.3096
$\gamma^h = 10$	0.3799	0.7973	1.2296	1.6753	2.2981

parameters. As before, we explore MT dynamics by determining the catastrophe frequency and the total pause duration as each of the above aforementioned parameters are increased in turn.

In Table 7, for fixed pause transition number $N_{tr} = 1.5$ and varying shortening rate δ (see column highlighted in yellow in Table 7) there is little to no change in the catastrophe frequency. Similarly, for fixed $N_{tr} = 1.5$ and varying δ (see highlighted column again in Table 8), MTs remain in the paused state for the same duration. In general, as the pause transition number is increased, this trend remains the same, with catastrophe frequencies and pause duration remaining fixed in each column.

As stated previously, MT destabilizing drugs work to increase MT catastrophe frequency and promote depolymerization (Stanton et al., 2011). We had assumed that an increase in the depolymerization parameter would increase MT depolymerization, but this was not the case. We leave a few thoughts about why this might be in the Discussion and Conclusion Section.

Finally we explore the catastrophe frequency and the total pause duration as we vary the transition number N_{tr} and the hydrolysis rate γ^h . We note that for fixed values of N_{tr} (e.g., $N_{tr} = 1.5$) (see column highlighted in pink in Table 9) that the catastrophe frequency increases as we increase the hydrolysis rate, a result that has been theorized and tested by Gardner et al. (2011). In addition, we note that for a fixed value of $N_{tr} = 1.5$ (see column highlighted in pink in Table 10) that the pause duration also decreases with increasing hydrolysis. Both of these results are consistent with those illustrated in Fig. 6. In particular, we note increased oscillations in the tubulin concentration curves as hydrolysis increases, which illustrates an increase in MT dynamical instability, and hence an increase in the catastrophe frequency. Finally, we also note an increase in the free-GTP tubulin population, and a corresponding decrease in the polymerized tubulin populations as hydrolysis is increased, illustrating MT depolymerization. As stated above, an increase in catastrophe frequency and MT depolymerization are both characteristics of MT destabilizing drugs (like the vinca alkaloids), and hence an effect of these destabilizing drugs could be an implicit action that triggers an increase in the MT hydrolysis rate, perhaps for increasing drug concentrations.

4. Conclusions and discussion

In this work, we developed a new mathematical model, based on an extensions of the work by White et al. (2017) and Hinow et al. (2009), to describe MT dynamic instability which takes into account not only growth and shortening, but also MT pause, a state that to our knowledge has not been studied from a theoretical framework before. New work by Shant et al. has shown, through high resolution microscopy, that the classical two-state model of growth and shortening does not adequately describe the more robust dynamics of MTs, in particular the existence of a paused state (Mahserejian et al., 2022).

To incorporate pause, a new model parameter C that describes a transition frequency into the paused state is included in the model. More specifically, C describes the total number of transitions that MTs make into the paused state from the growing state over the time course of the simulation. Although transition of MTs into paused states from

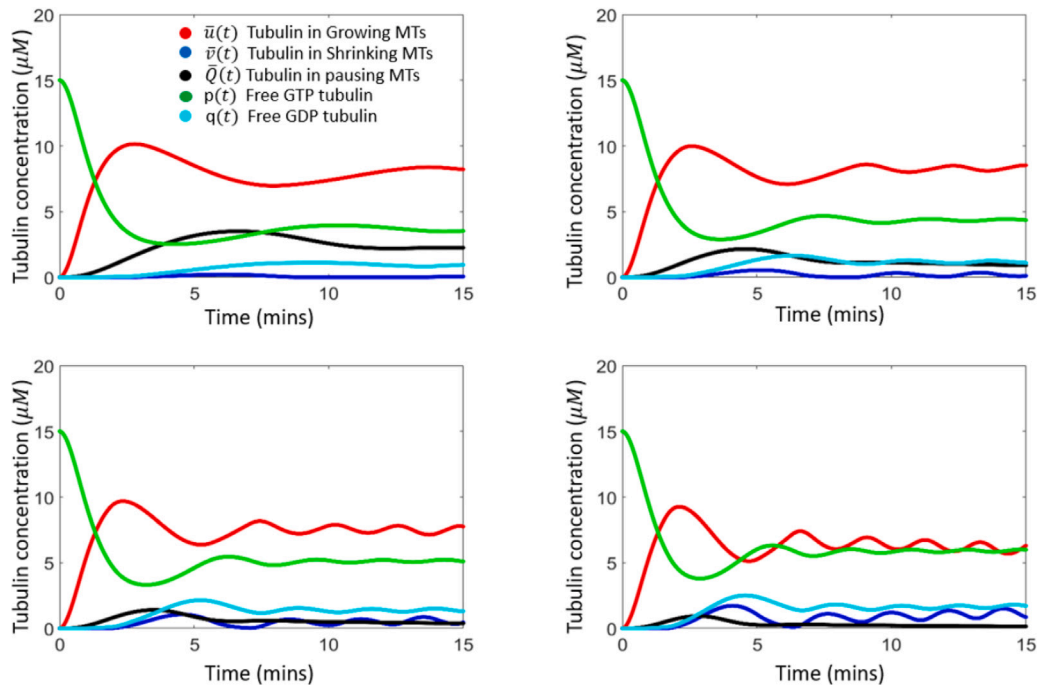


Fig. 6. Time evolution of tubulin in polymerized and free tubulin for variation in the hydrolysis rate γ^h holding N_{tr} at 1.5. From the top left to the bottom right, we have $\gamma^h = 4, 6, 8, 10 \mu\text{m min}^{-1}$. As the hydrolysis rate γ^h increases, we see an increase in the number of oscillations. This is indicative of an increase in the catastrophe frequency. Depolymerization is illustrated by the increase of free-GTP and free-GDP tubulin populations (and subsequent decreases in polymerized tubulin in both the growth and paused states).

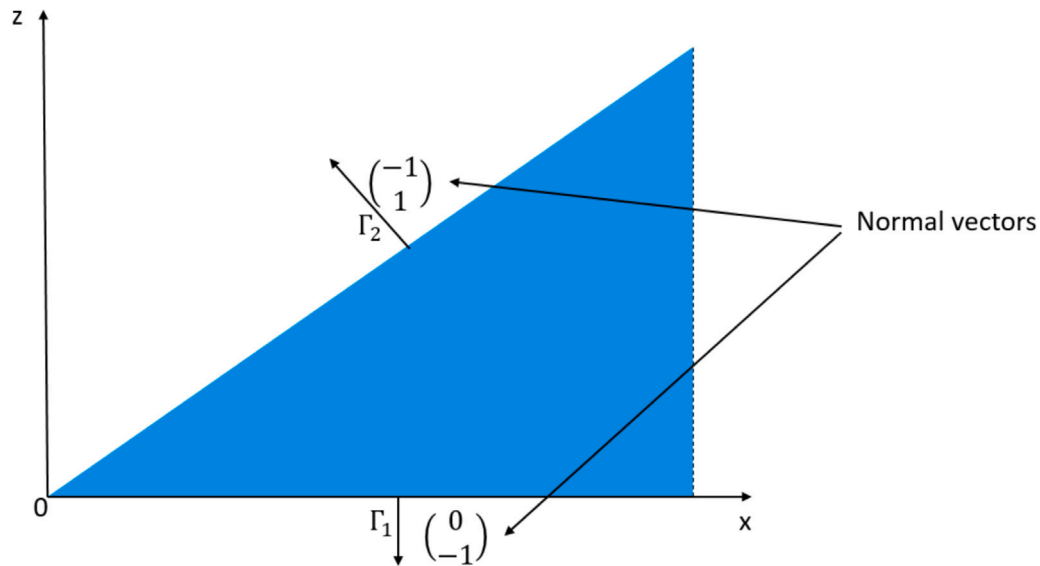


Fig. 7. Representation of the state space for MTs with boundaries Γ_1 and Γ_2 . Γ_1 represents the rescue boundary, where MTs without GTP caps are rescued, with the outer normal vector $\begin{pmatrix} 0 \\ -1 \end{pmatrix}$. Γ_2 represents the nucleation boundary and MTs cannot grow past this boundary. This has the outer normal vector $\begin{pmatrix} -1 \\ 1 \end{pmatrix}$.

shortening states has also been observed (Mahserejian et al., 2022), we leave this to a future work.

In addition to our new modeling framework, we have derived a mathematical expression for time-based MT catastrophe frequency in the presence of pause. In our modeling framework, the MT shortening rate, the growth parameter, and the MT rescue frequency are all model inputs, and so we explore the dynamics of our system by (1) calculation of the catastrophe frequency and (2) calculation of the duration of time MTs spend in a paused state. We used these calculations to understand how increases in certain model parameters associated with MT stabilization (like the MT growth rate parameter α), and MT destabilization

(like the MT shortening rate δ and the hydrolysis rate γ^h) alter MT dynamics in terms of changes to the catastrophe frequency and pause duration. Here, we assume that increases in the new pause transition number N_{tr} will have stabilizing properties (recall $N_{tr} = C \times T_{sim}$ where T_{sim} is the total simulation time).

By increasing parameters we thought to have stabilizing and destabilizing properties, we gained qualitative information into how the addition of various stabilizing MAPs, and stabilizing and destabilizing chemotherapeutic drugs (that target MTs) might act (directly or indirectly) on such parameters to alter their dynamics in their presence. In particular, increases in the growth rate parameter α and the

pause transition number N_{tr} had a stabilizing affect (representative of both stabilizing MAPs and stabilizing drugs) of decreasing catastrophe frequency and increasing pause duration. However, each parameter had distinct effects on polymerization; increases in N_{tr} led to smaller concentrations of tubulin in polymer form, whereas increases in α led to roughly similar sized polymer tubulin concentrations, results that compare to stabilizing drugs (like taxans), and stabilizing MAPs (like +TIPs), respectively.

We also explored the effects of increases in the shortening rate δ and the hydrolysis rate γ^h on MT dynamics. We noticed no change in our dynamic parameters when varying the shortening rate δ . In particular, for fixed pause transition number N_{tr} , there is no change in the catastrophe frequency or the pause duration for increasing δ . However, we did find that increases in the hydrolysis rate γ^h correspond to increases in the catastrophe frequency and decreases in the pause duration, in addition to increases in both free-GTP and free-GDP tubulin populations (indicative of increased depolymerization). Such results are comparable to destabilizing MT targeting drugs like those of the vinca alkaloid family and colchicine, which have the property that they depolymerize MTs at moderate to high concentrations and work to increase the catastrophe frequency.

Overall, we have extended on classical two state models of MT dynamics that include only growth and shortening by also considering MT pausing. Such considerations are important as pausing has been observed in MT systems, and even with this single theoretical approach we have observed that MTs dynamics are altered with its addition (recall the increase of MT catastrophe from near zero in Fig. 3 (again this was for a single set of model parameters but this qualitative feature was robust to parameter variations)).

In the future, it would be interesting to incorporate other pausing transitions, in addition to the pausing from growth and then shortening transition that we studied here. In particular, it would be interesting to study the other transitions that have been observed (Mahserejian et al., 2022), which include pausing from growing states back to growing states, pausing from shortening states back to shortening states, and pausing from shortening states back to growing states.

CRedit authorship contribution statement

Frederick Laud Amoah-Darko Jr.: Simulations, Figures, Modeling, Writing. **Diana White:** Conceptualization, Modeling, Writing, Interpretation of results.

Declaration of competing interest

The authors declare that they have no known competing financial interests or personal relationships that could have appeared to influence the work reported in this paper.

Data availability

No data was used for the research described in the article.

Appendix. Conversion of PDE to ODE (tubulin conservation)

The given system of equations [(2), (3), (4), (11), and (12)] conserves the total amount of tubulin in the MT system (i.e., all tubulin in growing, shortening, pausing, and free-tubulin states is conserved). We show this conservation here.

Let us consider the state space $\Sigma = \{(x, z) \in \mathbb{R}^2 : x \geq z \geq 0\}$ with boundaries $\Gamma_1 = \{(x, z) \in \Sigma : z = 0\}$ and $\Gamma_2 = \{(x, z) \in \Sigma : x = z\}$ as shown in Fig. 7.

Also, let $\mathbf{B} = \begin{pmatrix} \gamma^{poly}u \\ R(t)u \end{pmatrix}$ where $R(t) = \gamma^{poly}(p(t)) - \gamma^h$. Then Eq. (2) can be written as

$$\frac{\partial u}{\partial t} + \nabla \cdot \mathbf{B} = -cu \tag{26}$$

where $\nabla = (\partial/\partial x, \partial/\partial z)$. We now multiply Eq. (26) by x and integrate over the state space. We do this by using the divergence theorem for weighted integrals. We consider the outer normal \mathbf{n} which will be $\begin{pmatrix} 0 \\ -1 \end{pmatrix}$

on Γ_1 and $\begin{pmatrix} -1 \\ 1 \end{pmatrix}$ on Γ_2 so that the integration gives

$$\begin{aligned} \int_{\Sigma} x \frac{\partial u}{\partial t} dz dx &= - \int_{\Sigma} \nabla \cdot \mathbf{B} x dz dx - c\bar{u} \\ &= \int_{\Gamma_1} R(t)u(x, 0, t)x dx \\ &\quad + \int_{\Gamma_2} [\gamma^{poly} - \gamma^{poly} + \gamma^h] u(x, x, t)x dz dx \\ &\quad + \int_0^{\infty} \int_0^x \gamma^{poly} u(x, z, t) dz dx - c\bar{u}. \end{aligned}$$

This implies, after interchanging the order of differentiation and integration, that

$$\begin{aligned} \frac{d\bar{u}}{dt} &= \begin{cases} \int_0^{\infty} \lambda v(x, t)x dx & \text{if } R(t) \geq 0 \\ R(t) \int_0^{\infty} u(x, 0, t)x dx & \text{if } R(t) < 0 \end{cases} \\ &\quad + \int_0^{\infty} \frac{\mu}{L^*} p^2(t) \xi(x)x dx + \int_0^{\infty} \int_0^x \gamma^{poly} u(x, z, t) dz dx - c\bar{u}. \end{aligned}$$

where L^* is as defined in Eq. (7). Putting Eq. (7) into the second term on the right and side gives

$$\begin{aligned} \frac{d\bar{u}}{dt} &= \begin{cases} \int_0^{\infty} \lambda v(x, t)x dx & \text{if } R(t) \geq 0 \\ R(t) \int_0^{\infty} u(x, 0, t)x dx & \text{if } R(t) < 0 \end{cases} + \mu p^2(t) \\ &\quad + \int_0^{\infty} \int_0^x \gamma^{poly} u(x, z, t) dz dx - c\bar{u}. \end{aligned}$$

Similarly, we multiply Eq. (3) by x and integrate over x to give

$$\frac{d\bar{v}}{dt} - \delta \int_0^{\infty} x \frac{\partial v}{\partial x} dx = - \begin{cases} \lambda \int_0^{\infty} v(x, t)x dx & \text{if } R(t) \geq 0 \\ R(t) \int_0^{\infty} u(x, 0, t)x dx & \text{if } R(t) < 0. \end{cases}$$

We integrate the second term on the left side of the equation above by parts to obtain

$$\frac{d\bar{v}}{dt} = - \begin{cases} \lambda \int_0^{\infty} v(x, t)x dx & \text{if } R(t) \geq 0 \\ R(t) \int_0^{\infty} u(x, 0, t)x dx & \text{if } R(t) < 0 \end{cases} - \delta \int_0^{\infty} v(x, t) dx.$$

Now, multiply Eq. (4) by x and integrate over the state space. This gives

$$\begin{aligned} \frac{d\bar{Q}}{dt} &= \gamma^h \int_0^{\infty} \int_0^x \frac{\partial Q(x, z, t)}{\partial z} x dz dx + c\bar{u} \\ &= \gamma^h \int_0^{\infty} [Q(x, x, t) - Q(x, 0, t)] dx + c\bar{u} \\ &= -\gamma^h \int_0^{\infty} x Q(x, 0, t) dx + c\bar{u} \end{aligned}$$

So the complete ODE system is given as

$$\begin{aligned} \frac{d\bar{u}}{dt} &= \begin{cases} \lambda \int_0^{\infty} v(x, t)x dx & \text{if } R(t) \geq 0 \\ R(t) \int_0^{\infty} u(x, 0, t)x dx & \text{if } R(t) < 0 \end{cases} + \mu p^2(t) \\ &\quad + \gamma^{poly} \int_0^{\infty} \int_0^x u(x, z, t) dz dx - c\bar{u} \\ \frac{d\bar{v}}{dt} &= - \begin{cases} \lambda \int_0^{\infty} v(x, t)x dx & \text{if } R(t) \geq 0 \\ R(t) \int_0^{\infty} u(x, 0, t)x dx & \text{if } R(t) < 0 \end{cases} - \delta \int_0^{\infty} v(x, t) dx \\ \frac{d\bar{Q}}{dt} &= -\gamma^h \int_0^{\infty} Q(x, 0, t)x dx + c\bar{u} \\ \frac{dp}{dt} &= -\gamma^{poly}(p) \int_0^{\infty} \int_0^x u(x, z, t) dz dx - \mu p^n + \kappa q \\ \frac{dq}{dt} &= \delta \int_0^{\infty} v(x, t) dx - \kappa q + \gamma^h \int_0^{\infty} Q(x, 0, t)x dx \end{aligned}$$

Adding these equations together gives

$$\frac{d}{dt} [\bar{v}(t) + \bar{u}(t) + q(t) + p(t) + \bar{Q}(t)] = 0,$$

showing that the total concentration of tubulin is conserved.

References

- Aureliana Sousa, P.S., Reis, R., Sunkel, C.E., 2007. The drosophila CLASP homologue, mast/orbit regulates the dynamic behaviour of interphase microtubules by promoting the pause state. *Cell Motil. Cytoskeleton* 64, 605–620.
- Barlukova, A., White, D., Henry, G., Honore, S., Hubert, F., 2018. Mathematical modeling of microtubule dynamic instability: new insight into the link between GTP-hydrolysis and microtubule aging. *ESAIM: Math. Model. Numer. Anal.* 52, 2433–2456.
- Berges, R., Baeza-Kalleg, N., Tabouret, E., Chinot, O., Petit, M., Kruczynski, A., Figarella-Branger, D., Honore, S., Braguer, D., 2014. End-binding 1 protein overexpression correlates with glioblastoma progression and sensitizes to vinca-alkaloids in vitro and in vivo. *Oncotarget* 5 (24), 1–19.
- Bowne-Anderson, H., Zanicy, M., Kauer, M., Howard, J., 2013. Microtubule dynamic instability: A new model with coupled GTP hydrolysis and multistep catastrophe. *BioEssays* 35, <http://dx.doi.org/10.1002/bies.201200131>.
- Brittle, A.L., Ohkura, H., 2005. Mini spindles, the XMAP215 homologue, suppresses pausing of interphase microtubules in *Drosophila*. *EMBO J.* 24, 1387–1396.
- Chen, Y., Hill, T., 1985. Monte Carlo study of the GTP cap in a five-start helix model of a microtubule. *Proc. Natl. Acad. Sci. USA* 82, 1131–1135.
- de Forges, H., Pilon, A., Cantaloube, I., Pallandre, A., Haghiri-Gosnet, A.M., Perez, F., Poüs, C., 2016. Localized mechanical stress promotes microtubule rescue. *Curr. Biol.* 26, 3399–3406.
- Desai, A., Mitchison, T., 1997. Microtubule polymerization dynamics. *Annu. Rev. Cell Dev. Biol.* 13, 83–117.
- Dogterom, M., Leibler, S., 1993. Physical aspects of the growth and regulation of microtubule structures. *Phys. Rev. Lett.* 70, 1347–1350.
- Ebbinghaus, M., Santen, L., 2011. Theoretical modeling of aging effects in microtubule dynamics. *Theor. Model. Aging Effects Microtubule Dyn.* 100, 832–838.
- Etienne-Manneville, S., 2013. Microtubules in cell migration. *Cell Dev. Biol.* 29, 471–499.
- Fees, C., Moore, J., 2019. A unified model for microtubule rescue. *Mol. Biol. Cell* 30, 753–765.
- Flyvbjerg, H., Holy, T., Leibler, S., 1994. A model for caps and catastrophes. *Phys. Rev. Lett.* 73, 2372–2375.
- Flyvbjerg, H., Holy, T., Leibler, S., 1996. Microtubule dynamics: caps, catastrophes, and coupled hydrolysis. *Phys. Rev. Lett.* E 54, 5538–5560.
- Gardner, M., Zanic, M., Gell, C., Bormuth, V., Howard, J., 2011. The depolymerizing kinesins kip3 (kinesin-8) and mcak (kinesin-13) are catastrophe factors that destabilize microtubules by different mechanisms. *Nature Cell Biol.* 147 (5), 1092–1103.
- Hamel, E., del Campo, A., Lowe, M., C.M., L., 1981. Interactions of taxol, microtubule-associated proteins, and guanine nucleotides in tubulin polymerization. *J. Biol. Chem.* 256, 11887–11894.
- Hinow, P., Rezaia, V., Tuszynski, J., 2009. Continuous model for microtubule dynamics with catastrophe, rescue, and nucleation processes. *Phys. Rev. E* 80, <http://dx.doi.org/10.1103/PhysRevE.80.031904>.
- Honoré, S., Braguer, D., 2011. Investigating microtubule dynamic instability using microtubule-targeting agents. *Methods Mol. Biol.* 777, 245–260.
- Honore, S., Hubert, F., Tournus, M., White, D., 2019. A growth-fragmentation approach for modeling microtubule dynamic instability. *Bull. Math. Biol.* 81, 722–758.
- Janson, M., de Dood, M., Dogterom, M., 2003. Dynamic instability of microtubules is regulated by force. *J. Cell Biol.* 23, 1029–1034.
- Kumar, N., 1981. Taxol-induced polymerization of purified tubulin. Mechanism of action. *J. Biol. Chem.* 256, 10435–10441.
- Mahserejian, S., Scripture, J., Mauro, A., Lawrence, E., Jonasson, E., Murray, K., Li, J., Gardner, M., Alber, M., Zanic, M., Goodson, H., 2022. Quantification of microtubule stutters: dynamic instability behaviors that are strongly associated with catastrophe. *Mol. Biol. Cell* 33, 1–26.
- Martin, S., Schilstra, M., Bayley, P., 1993. Dynamic instability of microtubules: Monte Carlo simulation and application to different types of microtubule lattice. *Biophys. J.* 65, 578–596.
- Mirigian, M., Mukherejee, K., Bane, S., Sackett, D., Measurement of in vitro microtubule polymerization by turbidity and fluorescence. *Methods Cell Biol.* 115, 215–228.
- Mishra, P., Kunwar, A., Mukherji, S., Chowdhury, D., 2005. Dynamic instability of microtubules: Effect of catastrophe-suppressing drugs. *Phys. Rev. Lett.* E 72, DOI:051914.
- Moriwaki, T., Goshima, G., 2016. Five factors can reconstitute all three phases of microtubule polymerization dynamics. *J. Cell Biol.* 215 (3), 357–368.
- Pagano, A., Honore, S., Mohan, R., Berges, R., Akhmanova, A., 2012. Etoposide b inhibits migration of glioblastoma cells by inducing microtubule catastrophes and affecting ebl1 accumulation at microtubule plus ends. *Biochem. Pharmacol.* 84, 432–443.
- Sept, D., Limbach, H., Bolterauer, H., Tuszynski, J., 1999. A chemical kinetics model for microtubule oscillations. *J. Theoret. Biol.* 197, 77–88.
- Stanton, R.A., Gernert, K.M., Nettles, J.H., Aneja, R., 2011. Drugs that target dynamic microtubules: A new molecular perspective. *Med. Res. Rev.* 31, 443–481.
- Trogden, K., Rogers, S., 2015. TOG proteins are spatially regulated by Rac-GSK3beta to control interphase microtubule dynamics. *PLoS One* 1–25.
- van Riel, W., Rai, A., S. Bianchi, E.K., Q. Liu, A.J.H., Hoogenraad, C., Steinmetz, M., Kapitein, L., Akhmanova, A., 2017. Kinesin-4 KIF21B is a potent microtubule pausing factor. *ELIFE* e24746, <http://dx.doi.org/10.7554/eLife.24746.001>.
- Wade, R., 2009. On and around microtubules: An overview. *Mol. Biotechnol.* 43, 177–191.
- Walker, R., O'Brien, E., Pryer, N., Soboeiro, M., Voter, W., Erickson, H., Salmon, E., 1988. Dynamic instability of individual microtubules analyzed by video light microscopy: Rate constants and transition frequencies. *J. Cell Biol.* 107, 1437–1448.
- White, D., Honore, S., Hubert, F., 2017. Exploring the effect of end-binding proteins and microtubule targeting chemotherapy drugs on microtubule dynamic. *J. Theoret. Biol.*
- Wollman, R., Cytrynbaum, E., Jones, T., Meyer, T., Scholey, J., Mogilner, A., 2005. Efficient chromosome capture requires a bias in the search-and-capture process during mitotic-spindle assembly. *Curr. Biol.* 15, <http://dx.doi.org/10.1016/j.cub.2005.03.019>.
- Zauderer, E., 2006. *Partial Differential Equations of Applied Mathematics*, third ed. John Wiley and Sons, Inc., New Jersey.
- Zhou, J., Giannakakou, P., 2005. Targeting microtubules for cancer chemotherapy. *Curr. Med. Chem.* 5, 65–71.